



GoSam 2.0: Automated one loop calculations within and beyond the Standard Model

Nicolas Greiner^{a,b}

^a*Max-Planck-Institut für Physik, Föhringer Ring 6, 80805 München, Germany*

^b*DESY Theory Group, Notkestr. 85, D-22607 Hamburg, Germany*

Abstract

We present GoSam 2.0, a fully automated framework for the generation and evaluation of one loop amplitudes in multi leg processes. The new version offers numerous improvements both on generational aspects as well as on the reduction side. This leads to a faster and more stable code for calculations within and beyond the Standard Model. Furthermore it contains the extended version of the standardized interface to Monte Carlo programs which allows for an easy combination with other existing tools. We briefly describe the conceptual innovations and present some phenomenological results.

Keywords: NLO, Automation, QCD, BSM

1. Introduction

Two of the main challenges for the upcoming run 2 of the LHC will be a more precise determination of the Higgs [1, 2] properties and its couplings to bosons and fermions as well as the continued searches for new physics.

Both cases require a precise prediction for both signal and background processes. This particularly includes the calculation of next-to-leading order corrections in QCD. One of the main bottlenecks of such a computation is the calculation of the virtual one loop amplitude. The complexity and the need for having reliable tools for a large variety of different processes has led to the development of multi-purpose automated tools. An example of such a tool is the GoSam package [3] that focuses on the efficient generation and numerical evaluation of one loop amplitudes. The continuous refinement and extension of the existing package has led to the publication of the version 2.0 [4]. In this talk we will describe the improvements and new features contained in the the new version and present selected results that

have been obtained with GoSam 2.0.

2. New features in GoSam 2.0

2.1. Improvements in code generation

2.1.1. Code optimisation with FORM

GoSam generates an algebraic expression for each amplitude which is written in a Fortran90 file. It is obvious that the time needed to evaluate a single phase space point is highly dependent on how optimised the expression is written. In the first version the generation of an optimised expression has been done with the help of haggies [5]. In the new version we make use of new features provided by FORM version 4.x [6]. The new features result in a more compact code and a gain in speed of up to an order of magnitude.

2.1.2. Summing of diagrams with common subdiagrams

In order to improve the efficiency and the evaluation time, GoSam 2.0 is able to automatically sum algebraically diagrams that exhibit a similar structure to

a ‘meta-diagram’, which is then treated as a single diagram. In particular, diagrams that differ only by a propagator, which is not in the loop (e.g. Z vs. γ), are summed. Also diagrams with the same loop, but with a different external tree part are summed up. In the same way, diagrams, that share the same set of loop propagators but with different particle content in the loop, are combined to a single diagram.

This summing is controlled by the option `diagsum`, which is set to `True` by default.

2.1.3. Numerical polarisation vectors

To reduce the size of the code, numerical polarisation vectors are used for massless gauge bosons. This means that an algebraic expression is only written for a minimal set of helicity combinations and not for each combination separately. Per default this option is used, however it can be switched off by setting `polvec=explicit`.

2.2. Improvements in the reduction

2.2.1. New reduction method

The default reduction method in GoSam 2.0 is NINJA [7, 8, 9]. It is a further improvement of the integrand reduction method [10, 11, 12], based on the idea, that the coefficients of the residues of a loop integral can be extracted in a more efficient way by performing a Laurent expansion of the integrand. This methods requires less numerical sampling and therefore leads to a faster and more stable reduction.

2.2.2. Higher rank integrals

The tensor integral of a one loop calculation can be written in a very general form as

$$I_N^{\mu_1 \dots \mu_r}(S) = \int d^n k \frac{k^{\mu_1} \dots k^{\mu_r}}{\prod_{i=1}^N ((k + r_i)^2 - m_i^2 + i\delta)} \quad (1)$$

In the Standard Model the maximal value for r is $r = N$. However, in BSM theories and effective theories, larger values for r can occur. Therefore, the libraries NINJA [7, 8, 9], GOLEM95 [13, 14, 15, 16] and SAMURAI [17] have been extended to deal with the case of $r = N + 1$. This is an important ingredient for Higgs production in gluon fusion which we discuss later.

2.2.3. The derive extension

The new version contains an improved tensorial reconstruction, based on the idea that the numerator can

be Taylor expanded around $q = 0$,

$$\begin{aligned} \mathcal{N}(q) &= \mathcal{N}(0) \\ &+ q^\mu \frac{\partial}{\partial q_\mu} \mathcal{N}(q)|_{q=0} \\ &+ \frac{1}{2!} q^\mu q^\nu \frac{\partial}{\partial q_\mu} \frac{\partial}{\partial q_\nu} \mathcal{N}(q)|_{q=0} + \dots \end{aligned} \quad (2)$$

This allows to read off the coefficients of the tensor integrals. It leads to a further improvement of the speed and the precision of the tensorial reconstruction.

2.2.4. Electroweak scheme choices

There are a various number of electroweak schemes, depending on which parameters are used as input parameters and which parameters are derived from the input parameters. A consistent treatment requires that a minimal set of input parameters are given, and all other parameters are then derived. GoSam 2.0 allows to choose all possible sets of consistent schemes and the remaining parameters are then automatically derived.

2.2.5. Rescue system

The new release contains a rescue system to automatically detect and rescue numerically unstable points. Unstable points are triggered by an insufficient cancellation of infrared poles. Several checks and re-evaluation with different reduction methods can then be performed. For further details, see Refs. [4, 8].

2.3. New ranges of applicability

2.3.1. Color- and spin-correlated matrix elements

The use of subtraction methods for NLO calculations require the calculation of color- and spin-correlated matrix elements, i.e. born-like matrix elements with either a modified color structure or the combination of amplitudes where the helicity of one external leg is flipped. The color correlated matrix elements are defined as

$$C_{ij} = \langle \mathcal{M} | \mathbf{T}_i \mathbf{T}_j | \mathcal{M} \rangle, \quad (3)$$

and the spin-correlated matrix element are defined as

$$S_{ij} = \langle \mathcal{M}, - | \mathbf{T}_i \mathbf{T}_j | \mathcal{M}, + \rangle. \quad (4)$$

Bot color- and spin-correlated matrix elements contain implicitly the sum over all helicities, only the helicities with the indices i and j are fixed, i.e.

$$\langle \mathcal{M}_{i,-} | \mathbf{T}_i \cdot \mathbf{T}_j | \mathcal{M}_{i,+} \rangle = \sum_{\lambda_1, \dots, \lambda_{i-1}, \lambda_{i+1}, \dots, \lambda_n} \langle \mathcal{M}_{\lambda_1, \dots, \lambda_{i-1}, -, \lambda_{i+1}, \dots, \lambda_n} | \mathbf{T}_i \cdot \mathbf{T}_j | \mathcal{M}_{\lambda_1, \dots, \lambda_{i-1}, +, \lambda_{i+1}, \dots, \lambda_n} \rangle. \quad (5)$$

In the new release, GoSam is able to generate these matrix elements and the information can be passed via the BLHA2 interface [18].

2.3.2. Complex mass scheme

A gauge invariant treatment of massive gauge bosons requires the use of the complex mass scheme, where the widths also enter in the definition of the weak mixing angle. The masses of the bosons are given by

$$m_V^2 \rightarrow \mu_V^2 = m_V^2 - im_V \Gamma_V, \quad V = W, Z. \quad (6)$$

In order to maintain gauge invariance this affects the definition of the Weinberg angle:

$$\cos \theta_W^2 = \frac{\mu_W^2}{\mu_Z^2}. \quad (7)$$

The complex mass scheme is implemented in GoSam via new models called `sm_complex` and `smdiaq_complex`, depending on whether one wants to use the full CKM matrix or a unit matrix.

3. Phenomenological applications

The new version GoSam 2.0 has been recently used in a sizeable number of challenging calculations of both within and beyond the Standard Model [19, 20, 21, 22, 23, 24, 25, 26, 27, 28, 29, 30]. In this talk we discuss the calculation of Higgs plus jets in gluon fusion and the calculation of a neutralino pair in association with a jet in the MSSM.

3.1. Higgs plus jets in gluon fusion

The gluon fusion channel is the dominant production mechanism of a Standard Model Higgs at the LHC. Even if one is interested in the vector boson fusion channel the gluon fusion mechanism is an irreducible background and therefore its precise determination is mandatory. In particular we have calculated the NLO QCD corrections to $H + 2$ [20] and $H + 3$ [22], and a comparison between the two processes has been studied in Ref. [30]. For the $H + 2$ jets process the results have been obtained by interfacing GoSam with Sherpa [31] via the BLHA interface [32]. In the case of $H + 3$ jets we have used MadGraph [33, 34] for the real emission matrix element, and MadDipole [35, 36] for the generation of the dipoles and the integrated subtraction terms. The phase space integration for these pieces has been performed using MadEvent [37], for the tree-level contribution and the integration of the virtual amplitude we have again used Sherpa.

We have obtained the numerical results with a basic setup of 8 TeV center of mass energy, basic cuts on the jets with $p_T > 30$ GeV, $\eta < 4.4$ and an anti-kt jet algorithm [38, 39] of $R = 0.4$. Renormalization- and factorization scales have been chosen to be equal and set to

$\mu_F = \mu_R = \frac{\hat{H}_T}{2} = \frac{1}{2} \left(\sqrt{m_H^2 + p_{T,H}^2} + \sum_i |p_{T,i}| \right)$. For the LO PDFs we have used the cteq611 pdf set, for the NLO PDFs we have used the ct10nlo pdf set.

The main results on the level of total cross sections are summarized in Table 1. Both processes show a sizeable global K-factor of roughly 1.3 which stresses the importance of including the NLO QCD corrections. The K-factor increases if NLO PDFs are used for both LO and NLO calculation. One interesting aspect is the fact that if one looks at the ratios of the total cross sections of $H+3$ over $H+2$ they show, they are to a very good approximation constant, independent whether one looks at the ratio of LO cross sections with LO or NLO pdfs or at NLO cross sections.

The comparison between the two processes allows to assess the effects of the additional jet on Higgs observables. Two examples are shown in Fig.1, namely the rapidity and the p_T distribution of the Higgs. Looking at the ratios allows us to assess the effect of the third jet on the observables. The ratio plots are normalized to the $H + 2$ result. One can see that the rapidity distribution is rather insensitive to the radiation of an additional jet, whereas the p_T distribution shows a clear increase of the importance of the third jet on the Higgs p_T in the high- p_T region. The reason for this increase is a mere phase space argument. A high p_T for the Higgs can be more easily obtained by distributing the necessary recoil p_T on three jets rather than on two. The high p_T phase space points are almost evenly distributed in rapidity space, therefore there is hardly any effect visible.

3.2. Neutralino pair production in association with a jet

An example for a highly non-trivial BSM process is the production of a pair of the lightest neutralinos in association with a jet [19]. We have calculated the Susy-QCD corrections to this process in the MSSM [19]. The neutralino is the LSP which makes this process lead to the simple experimental signature of missing energy and a mono-jet. From a calculational point of view it is a very challenging process as it contains several mass scales. And as full off-shell effects are taken into account one has to deal with a non-trivial resonance structure. The most complicated loop diagrams involve rank 3 pentagons 4 internal masses. Concerning the computational setup GoSam has been used for the generation of the virtual one loop amplitude. In order to deal with a certain model (SM, MSSM, etc.) GoSam requires the presence of a model file, that contains the Feynman rules of that model. Per default GoSam only contains model files for various versions of the Standard

| Sample K -factor | Cross sections for Higgs boson plus | | | |
|------------------------------|---------------------------------------|-------|---------------------------------------|---|
| | ≥ 2 jets | f_3 | ≥ 3 jets | $r_{3/2}$ |
| LO | | | | |
| $H+2$ -jet2 (LO PDFs) | 1.23 ^{+37%} _{-24%} | | | |
| $H+3$ -jets (LO PDFs) | (0.381) | 1.0 | 0.381 ^{+53%} _{-32%} | 0.310 ^{0.347} _{0.278} |
| ----- | | | | |
| $H+2$ -jets (NLO PDFs) | 0.970 ^{+33%} _{-23%} | | | |
| $H+3$ -jets (NLO PDFs) | (0.286) | 1.0 | 0.286 ^{+50%} _{-31%} | 0.295 ^{0.332} _{0.265} |
| NLO | | | | |
| $H+2$ -jets | 1.590 ^{-4%} _{-7%} | 0.182 | 0.289 ^{+49%} _{-31%} | |
| $H+3$ -jets | (0.485) | 1.0 | 0.485 ^{-3%} _{-13%} | 0.305 ^{0.307} _{0.284} |
| K_2, K_3 (LO PDFs for LO) | 1.29 ^{0.911} _{1.59} | | 1.27 ^{0.806} _{1.63} | |
| K_2, K_3 (NLO PDFs for LO) | 1.64 ^{1.19} _{1.98} | | 1.70 ^{1.10} _{2.13} | |

Table 1: Cross sections in pb for the various parton-level Higgs boson plus jet samples used in this study. The upper and lower parts of the table show the LO and NLO results, respectively, together with their uncertainties (in percent) from varying scales by factors of two, up (subscript position) and down (superscript position). NLO-to-LO K -factors, K_n , for both the inclusive 2-jets ($n = 2$) and 3-jets ($n = 3$) bin, the cross section ratio $r_{3/2}$ and m -jet fractions, f_m , are given in addition.

Model, however new models can easily be imported with the help of Feynrules [40] which can be used to write a model file in the UFO format [41]. A model file in this format is automatically understood by GoSam. For our studies we chose a pragmatic and experimentally motivated parameterisation of Susy, known as the phenomenological MSSM (pMSSM) [42, 43, 44], in a variant involving 19 free parameters (p19MSSM). The relevant Susy parameters are given in Table 2.

The calculation of the UV counter terms has been done separately. Tree-level and real emission matrix elements have been calculated using MadGraph, for the subtraction terms we have used MadDipole.

For processes involving unstable particles, the proper definition of the set of diagrams contributing to the next-to-leading order corrections is not obvious. There are problems of double counting as diagrams with additional real radiation from the unstable particle in the final state can, if it becomes resonant, also be regarded as part of a leading order process with the decay already included in the narrow width approximation. More specifically, in the real emission contribution there is the possibility of producing a squark pair, where the squarks decay into a quark and a neutralino. Close to the resonance, this contribution gets quite large, and in fact

| SUSY Parameters | |
|--------------------------------|-----------------------------------|
| $M_{\tilde{\chi}_1^0} = 299.5$ | $\Gamma_{\tilde{\chi}_1^0} = 0$ |
| $M_{\tilde{g}} = 415.9$ | $\Gamma_{\tilde{g}} = 4.801$ |
| $M_{\tilde{u}_L} = 339.8$ | $\Gamma_{\tilde{u}_L} = 0.002562$ |
| $M_{\tilde{u}_R} = 396.1$ | $\Gamma_{\tilde{u}_R} = 0.1696$ |
| $M_{\tilde{d}_L} = 348.3$ | $\Gamma_{\tilde{d}_L} = 0.003556$ |
| $M_{\tilde{d}_R} = 392.5$ | $\Gamma_{\tilde{d}_R} = 0.04004$ |
| $M_{\tilde{b}_L} = 2518.0$ | $\Gamma_{\tilde{b}_L} = 158.1$ |
| $M_{\tilde{b}_R} = 2541.8$ | $\Gamma_{\tilde{b}_R} = 161.0$ |
| $M_{\tilde{t}_L} = 2403.7$ | $\Gamma_{\tilde{t}_L} = 148.5$ |
| $M_{\tilde{t}_R} = 2668.6$ | $\Gamma_{\tilde{t}_R} = 182.9$ |

Table 2: Masses and widths of the supersymmetric particles for the benchmark point used. The second generation of squarks is degenerate with the first generation of squarks. All parameters are given in GeV.

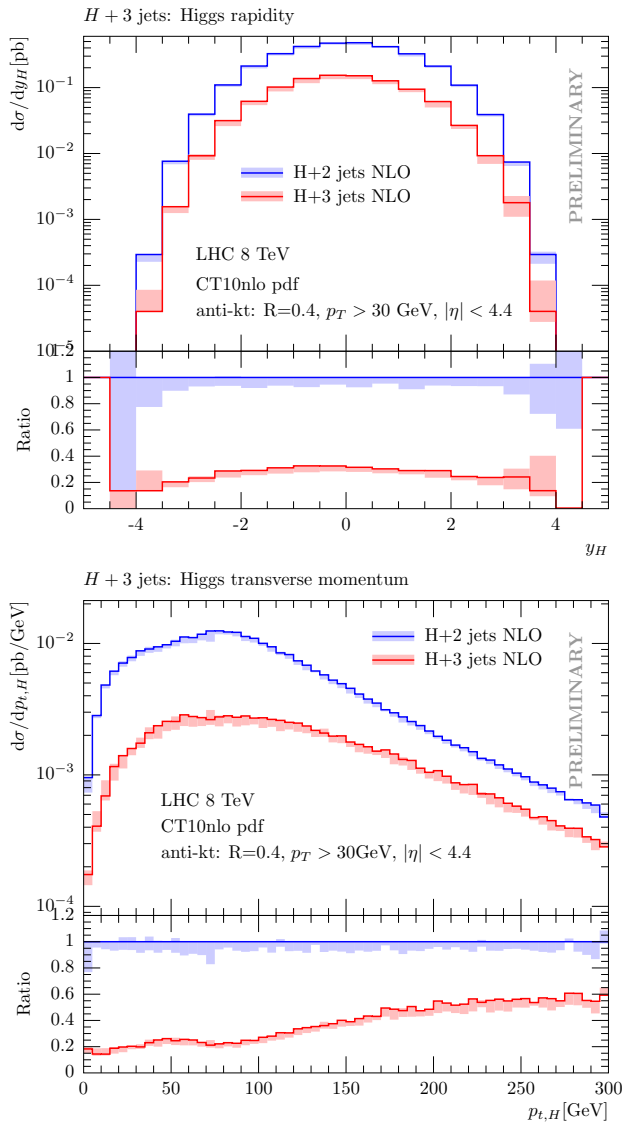


Figure 1: Rapidity and p_T -distribution of the Higgs for $H + 2$ and $H + 3$ at NLO. The ratios are normalized to the $H + 2$ result.

should rather be counted as a leading order contribution to squark pair production with subsequent squark decay, because here we are interested in the radiative corrections to the final state of a monojet in association with a neutralino pair.

Therefore the calculation was carried out in two different ways. In the first approach we take into account all possible diagrams leading to the required final state consisting of two neutralinos and two QCD partons. In particular this includes the possibility of having two on-shell squarks. In the second approach we remove the diagrams with two squarks in the s -channel from the

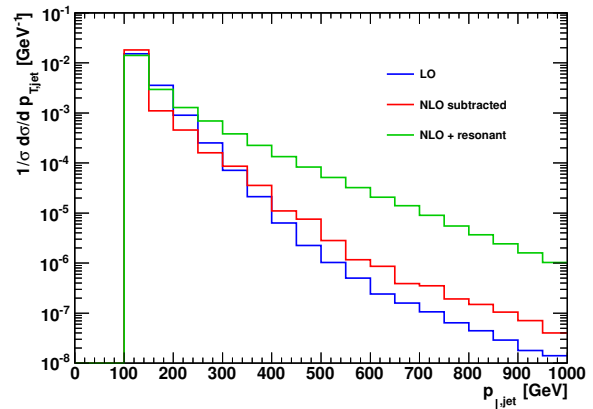


Figure 2: Normalized distributions showing the transverse momentum distribution of the leading jet at $\sqrt{s} = 8$ TeV, comparing the cases where the resonant diagrams are included to the ones where they are subtracted.

amplitude. In general, the removal of diagrams leads to a violation of gauge invariance, however one can show that gauge invariance is still preserved for a large class of gauges [19] or found to lead to a small effect only [45].

The difference between the two approaches in case of the p_T of the jet is shown in Fig. 2. The distribution is normalized to the total cross section. The curve in blue shows the distribution at leading order, the red curve shows the NLO distribution where the doubly resonant squark pair diagrams have been removed. The green curve shows the full result, also taking these resonant diagrams into account. As can be clearly seen these resonant diagrams lead to a huge enhancement spoiling the perturbative convergence. Subtracting the diagrams then leads to a well-behaved perturbative expansion. For a more detailed phenomenology of this process we refer to Ref. [19].

4. Conclusions

In this talk we have presented the new release of GoSam, which contains a multitude of improvements compared to the previous version. Refinements have been made in the context of diagram generation as well as on the reduction side, both leading to a substantial gain in generation time, size of the code and the time needed for the evaluation of a phase space point. New reduction mechanisms and a rescue system have led to a more stable and reliable performance. We have discussed the new features and as selected examples for recent phenomenological applications we presented the

calculations of Higgs plus jets in gluon fusion and the production of a neutralino pair plus one jet in the context of the MSSM.

5. Acknowledgments

We would like to thank the present and former members of the GoSam collaboration for their effort in the development of GoSam. Furthermore we would like to thank Joey Huston, Jan Winter and Valery Yundin for their collaboration and their work in the Higgs plus jets project.

References

- [1] G. Aad, et al., Observation of a new particle in the search for the Standard Model Higgs boson with the ATLAS detector at the LHC, *Phys.Lett. B* 716 (2012) 1–29. arXiv:1207.7214, doi:10.1016/j.physletb.2012.08.020.
- [2] S. Chatrchyan, et al., Observation of a new boson at a mass of 125 GeV with the CMS experiment at the LHC, *Phys.Lett. B* 716 (2012) 30–61. arXiv:1207.7235, doi:10.1016/j.physletb.2012.08.021.
- [3] G. Cullen, N. Greiner, G. Heinrich, G. Luisoni, P. Mastrolia, et al., Automated One-Loop Calculations with GoSam, *Eur.Phys.J. C* 72 (2012) 1889. arXiv:1111.2034, doi:10.1140/epjc/s10052-012-1889-1.
- [4] G. Cullen, H. van Deurzen, N. Greiner, G. Heinrich, G. Luisoni, et al., GoSam-2.0: a tool for automated one-loop calculations within the Standard Model and beyond, *Eur.Phys.J. C* 74 (2014) 3001. arXiv:1404.7096, doi:10.1140/epjc/s10052-014-3001-5.
- [5] T. Reiter, Optimising Code Generation with haggies, *Comput.Phys.Commun.* 181 (2010) 1301–1331. arXiv:0907.3714, doi:10.1016/j.cpc.2010.01.012.
- [6] J. Kuipers, T. Ueda, J. Vermaseren, J. Vollinga, FORM version 4.0, *Comput.Phys.Commun.* 184 (2013) 1453–1467. arXiv:1203.6543, doi:10.1016/j.cpc.2012.12.028.
- [7] P. Mastrolia, E. Mirabella, T. Peraro, Integrand reduction of one-loop scattering amplitudes through Laurent series expansion, *JHEP* 1206 (2012) 095. arXiv:1203.0291, doi:10.1007/JHEP11(2012)128, 10.1007/JHEP06(2012)095.
- [8] H. van Deurzen, G. Luisoni, P. Mastrolia, E. Mirabella, G. Ossola, et al., Multi-leg One-loop Massive Amplitudes from Integrand Reduction via Laurent Expansion, *JHEP* 1403 (2014) 115. arXiv:1312.6678, doi:10.1007/JHEP03(2014)115.
- [9] T. Peraro, Ninja: Automated Integrand Reduction via Laurent Expansion for One-Loop Amplitudes, *Comput.Phys.Commun.* 185 (2014) 2771–2797. arXiv:1403.1229, doi:10.1016/j.cpc.2014.06.017.
- [10] G. Ossola, C. G. Papadopoulos, R. Pittau, Reducing full one-loop amplitudes to scalar integrals at the integrand level, *Nucl.Phys. B* 763 (2007) 147–169. arXiv:hep-ph/0609007, doi:10.1016/j.nuclphysb.2006.11.012.
- [11] P. Mastrolia, G. Ossola, C. G. Papadopoulos, R. Pittau, Optimizing the Reduction of One-Loop Amplitudes, *JHEP* 0806 (2008) 030. arXiv:0803.3964, doi:10.1088/1126-6708/2008/06/030.
- [12] G. Ossola, C. G. Papadopoulos, R. Pittau, On the Rational Terms of the one-loop amplitudes, *JHEP* 0805 (2008) 004. arXiv:0802.1876, doi:10.1088/1126-6708/2008/05/004.
- [13] T. Binoth, J.-P. Guillet, G. Heinrich, E. Pilon, T. Reiter, Golem95: A Numerical program to calculate one-loop tensor integrals with up to six external legs, *Comput.Phys.Commun.* 180 (2009) 2317–2330. arXiv:0810.0992, doi:10.1016/j.cpc.2009.06.024.
- [14] G. Heinrich, G. Ossola, T. Reiter, F. Tramontano, Tensorial Reconstruction at the Integrand Level, *JHEP* 1010 (2010) 105. arXiv:1008.2441, doi:10.1007/JHEP10(2010)105.
- [15] G. Cullen, J. P. Guillet, G. Heinrich, T. Kleinschmidt, E. Pilon, et al., Golem95C: A library for one-loop integrals with complex masses, *Comput.Phys.Commun.* 182 (2011) 2276–2284. arXiv:1101.5595, doi:10.1016/j.cpc.2011.05.015.
- [16] J. P. Guillet, G. Heinrich, J. von Soden-Fraunhofen, Tools for NLO automation: extension of the golem95C integral library, *Comput.Phys.Commun.* 185 (2014) 1828–1834. arXiv:1312.3887, doi:10.1016/j.cpc.2014.03.009.
- [17] P. Mastrolia, G. Ossola, T. Reiter, F. Tramontano, Scattering AMplitudes from Unitarity-based Reduction Algorithm at the Integrand-level, *JHEP* 1008 (2010) 080. arXiv:1006.0710, doi:10.1007/JHEP08(2010)080.
- [18] S. Alioli, S. Badger, J. Bellm, B. Biedermann, F. Boudjema, et al., Update of the Binoth Les Houches Accord for a standard interface between Monte Carlo tools and one-loop programs, *Comput.Phys.Commun.* 185 (2014) 560–571. arXiv:1308.3462, doi:10.1016/j.cpc.2013.10.020.
- [19] G. Cullen, N. Greiner, G. Heinrich, Susy-QCD corrections to neutralino pair production in association with a jet, *Eur.Phys.J. C* 73 (2013) 2388. arXiv:1212.5154, doi:10.1140/epjc/s10052-013-2388-8.
- [20] H. van Deurzen, N. Greiner, G. Luisoni, P. Mastrolia, E. Mirabella, et al., NLO QCD corrections to the production of Higgs plus two jets at the LHC, *Phys.Lett. B* 721 (2013) 74–81. arXiv:1301.0493, doi:10.1016/j.physletb.2013.02.051.
- [21] T. Gehrmann, N. Greiner, G. Heinrich, Photon isolation effects at NLO in $\gamma\gamma$ + jet final states in hadronic collisions, *JHEP* 1306 (2013) 058. arXiv:1303.0824, doi:10.1007/JHEP06(2013)058, 10.1007/JHEP06(2013)058.
- [22] G. Cullen, H. van Deurzen, N. Greiner, G. Luisoni, P. Mastrolia, et al., Next-to-Leading-Order QCD Corrections to Higgs Boson Production Plus Three Jets in Gluon Fusion, *Phys.Rev.Lett.* 111 (13) (2013) 131801. arXiv:1307.4737, doi:10.1103/PhysRevLett.111.131801.
- [23] N. Greiner, G. Heinrich, J. Reichel, J. F. von Soden-Fraunhofen, NLO QCD Corrections to Diphoton Plus Jet Production through Graviton Exchange, *JHEP* 1311 (2013) 028. arXiv:1308.2194, doi:10.1007/JHEP11(2013)028.
- [24] T. Gehrmann, N. Greiner, G. Heinrich, Precise QCD predictions for the production of a photon pair in association with two jets, *Phys.Rev.Lett.* 111 (2013) 222002. arXiv:1308.3660, doi:10.1103/PhysRevLett.111.222002.
- [25] M. J. Dolan, C. Englert, N. Greiner, M. Spannowsky, Further on up the road: $hhjj$ production at the LHC, *Phys.Rev.Lett.* 112 (2014) 101802. arXiv:1310.1084, doi:10.1103/PhysRevLett.112.101802.
- [26] G. Luisoni, P. Nason, C. Oleari, F. Tramontano, HW^*/HZ + 0 and 1 jet at NLO with the POWHEG BOX interfaced to GoSam and their merging within MiNLO, *JHEP* 1310 (2013) 083. arXiv:1306.2542, doi:10.1007/JHEP10(2013)083.
- [27] S. Hoeche, J. Huang, G. Luisoni, M. Schoenherr, J. Winter, Zero and one jet combined next-to-leading order analysis of the top quark forward-backward asymmetry, *Phys.Rev. D* 88 (1) (2013) 014040. arXiv:1306.2703, doi:10.1103/PhysRevD.88.014040.
- [28] H. van Deurzen, G. Luisoni, P. Mastrolia, E. Mirabella, G. Ossola, et al., Next-to-Leading-Order QCD Corrections to Higgs Boson Production in Association with a Top Quark Pair and a

- Jet, Phys.Rev.Lett. 111 (17) (2013) 171801. arXiv:1307.8437, doi:10.1103/PhysRevLett.111.171801.
- [29] G. Heinrich, A. Maier, R. Nisius, J. Schlenk, J. Winter, NLO QCD corrections to $W^+W^-b\bar{b}$ production with leptonic decays in the light of top quark mass and asymmetry measurements, JHEP 1406 (2014) 158. arXiv:1312.6659, doi:10.1007/JHEP06(2014)158.
- [30] J. Butterworth, G. Dissertori, S. Dittmaier, D. de Florian, N. Glover, et al., Les Houches 2013: Physics at TeV Colliders: Standard Model Working Group Report arXiv:1405.1067.
- [31] T. Gleisberg, S. Hoeche, F. Krauss, M. Schonherr, S. Schumann, et al., Event generation with SHERPA 1.1, JHEP 0902 (2009) 007. arXiv:0811.4622, doi:10.1088/1126-6708/2009/02/007.
- [32] T. Binoth, F. Boudjema, G. Dissertori, A. Lazopoulos, A. Denner, et al., A Proposal for a standard interface between Monte Carlo tools and one-loop programs, Comput.Phys.Commun. 181 (2010) 1612–1622. arXiv:1001.1307, doi:10.1016/j.cpc.2010.05.016.
- [33] T. Stelzer, W. Long, Automatic generation of tree level helicity amplitudes, Comput.Phys.Commun. 81 (1994) 357–371. arXiv:hep-ph/9401258, doi:10.1016/0010-4655(94)90084-1.
- [34] J. Alwall, P. Demin, S. de Visscher, R. Frederix, M. Herquet, et al., MadGraph/MadEvent v4: The New Web Generation, JHEP 0709 (2007) 028. arXiv:0706.2334, doi:10.1088/1126-6708/2007/09/028.
- [35] R. Frederix, T. Gehrmann, N. Greiner, Automation of the Dipole Subtraction Method in MadGraph/MadEvent, JHEP 0809 (2008) 122. arXiv:0808.2128, doi:10.1088/1126-6708/2008/09/122.
- [36] R. Frederix, T. Gehrmann, N. Greiner, Integrated dipoles with MadDipole in the MadGraph framework, JHEP 1006 (2010) 086. arXiv:1004.2905, doi:10.1007/JHEP06(2010)086.
- [37] F. Maltoni, T. Stelzer, MadEvent: Automatic event generation with MadGraph, JHEP 0302 (2003) 027. arXiv:hep-ph/0208156, doi:10.1088/1126-6708/2003/02/027.
- [38] M. Cacciari, G. P. Salam, G. Soyez, The Anti-k(t) jet clustering algorithm, JHEP 0804 (2008) 063. arXiv:0802.1189, doi:10.1088/1126-6708/2008/04/063.
- [39] M. Cacciari, G. P. Salam, G. Soyez, FastJet User Manual, Eur.Phys.J. C72 (2012) 1896. arXiv:1111.6097, doi:10.1140/epjc/s10052-012-1896-2.
- [40] N. D. Christensen, C. Duhr, FeynRules - Feynman rules made easy, Comput.Phys.Commun. 180 (2009) 1614–1641. arXiv:0806.4194, doi:10.1016/j.cpc.2009.02.018.
- [41] C. Degrande, C. Duhr, B. Fuks, D. Grellscheid, O. Mattelaer, et al., UFO - The Universal FeynRules Output, Comput.Phys.Commun. 183 (2012) 1201–1214. arXiv:1108.2040, doi:10.1016/j.cpc.2012.01.022.
- [42] A. Djouadi, J.-L. Kneur, G. Moultaka, SuSpect: A Fortran code for the supersymmetric and Higgs particle spectrum in the MSSM, Comput.Phys.Commun. 176 (2007) 426–455. arXiv:hep-ph/0211331, doi:10.1016/j.cpc.2006.11.009.
- [43] C. F. Berger, J. S. Gainer, J. L. Hewett, T. G. Rizzo, Supersymmetry Without Prejudice, JHEP 0902 (2009) 023. arXiv:0812.0980, doi:10.1088/1126-6708/2009/02/023.
- [44] S. AbdusSalam, B. Allanach, H. Dreiner, J. Ellis, U. Ellwanger, et al., Benchmark Models, Planes, Lines and Points for Future SUSY Searches at the LHC, Eur.Phys.J. C71 (2011) 1835. arXiv:1109.3859.
- [45] S. Frixione, E. Laenen, P. Motylinski, B. R. Webber, C. D. White, Single-top hadroproduction in association with a W boson, JHEP 0807 (2008) 029. arXiv:0805.3067, doi:10.1088/1126-6708/2008/07/029.